Design of a full silica pulse compression grating

Nicolas Bonod, J. Neauport

Design of a full silica pulse compression grating

Nicolas Bonod,[1] Jérôme Neauport,[2]

[1] *Institut Fresnel CNRS UMR6133 / Equipe Clarté, Domaine universitaire de St Jérôme, 13397 Marseille, France*

[2]*CEA Cesta, BP2, 33114 Le Barp, France*

[*]*Corresponding author: nicolas.bonod@fresnel.fr*

A diffraction grating engraved on a two-dimensional photonic crystal composed of square air holes in a silica matrix is numerically studied for the compression of ultra-short pulses. The silica is therefore the only solid material of the grating and the reflection of the incident beam is based on the contrast of the air and silica refractive indices. This optical component enables the single use of silica as a solid material presenting a high laser induced damage threshold. In comparison to gratings engraved on a dielectric stack (MLD), it offers the advantage of avoiding the presence of interfaces between 2 solid materials with different mechanical properties, sources of mechanical constraints which can distort the grating.

OCIS codes: (*140.7090) Lasers and laser optics: Ultrafast lasers, (050.1950)Diffraction and gratings*: *Diffraction gratings, (050.5298)Diffraction and gratings*: *Photonic crystals*

Diffraction gratings are used in the compression of ultra-short pulses amplified by the so-called « frequency drift » method or Chirped Pulse Amplification (CPA) [1]. Such diffraction gratings must offer a high diffraction efficiency to limit energy losses during pulse compression and a high laser induced damage threshold (LIDT) since the incident beam has been previously amplified, generally by a laser pumped titanium-sapphire crystal. Metal gratings can be used but their low LIDT requires a high angle of incidence and such gratings must therefore present a large surface area, resulting in disadvantages related to their weight and cost. Moreover, metal causes losses to the extent that the reflected efficiency is limited [2]. Entirely dielectric gratings appeared in the mid 1990's [3]. They made it possible to significantly increase the LIDT of compression gratings and to obtain measured reflected efficiencies close to 96% [4]. These diffraction gratings are engraved on a dielectric stack with 2 materials of high and low indices. Hafnium dioxide (HfO_2) and silica (SiO_2) are very frequently used. The disadvantage of this type of stacking lies in the presence of mechanical constraints at the interfaces due to the different mechanical properties of the two materials which can deform the mirror and distort the spatial qualities of the beam, and also considerably reduce the LIDT of the mirrors. Moreover, silica has with very good resistance to the laser flow but the other oxides frequently used, such as Ta_2O_5, HfO_2, Al_2O_3 and TiO_2, present much lower LIDT which tends to reduce the damage threshold of the mirror [5].

To overcome these problems posed by dielectric stacks, this paper presents a study of two-dimensional (2D) photonic crystals [6]. Air holes are made in a silica matrix which then acts as the high refractive index material whereas the air acts as the low refractive index material. These crystals avoid the use of a solid material other than silica and therefore eliminate the presence of interfaces between 2 solid materials. The period of the photonic crystal is small enough such that the 0th order is the only propagative order. The grating is engraved on the photonic crystal with a larger period than that of the photonic crystal to allow the propagation of the -1st dispersive order. As a consequence, the photonic crystal diffraction grating presents 2 different periods. The differential method is suited for modelling periodical devices, so that the period of the diffraction grating on the Ox axis (see figure 1) must be an integer of the period the photonic crystal. In this study, the period of the diffraction grating is chosen to be twice that of the photonic crystal [7-9].

This study refers to the opto-geometric parameters of the diffraction gratings used in the final stage of pulse compression of the PETAL project [10]. The wavelength is set at 1053 nm, the angle of incidence at 77.2°, polarization is Transverse Electric (TE) and the period is 562 nm. Air holes in silica have a square cross section for numerical convenience, but circular cross section would give similar results [11]. Their periodicity is fixed at one half of the periodicity of the grating, namely 281 nm (Figure 1). The length of the sides of the squares is denoted a, and the thickness between two layers of air holes along the Oy axis is denoted Δ. Calculations are performed by a numerical code based on the differential method [12]. Convergence is rapidly reached and ensured for all the results presented in this study.

The first stage of the study consists of defining the geometry of the photonic crystal to guarantee its all-but-perfect reflectivity. The angle of incidence equal to 70.9° is set at the median angle between the 2 angles of diffraction of the –1st and 0th orders of the diffraction grating that will be subsequently added to the photonic crystal [12-13]. The reflectivity of the crystal is thus calculated with respect to the length of the square cross section of air holes a and to the residual thickness Δ of silica between two layers of air holes (see Fig.1). Air holes with a side length of 0.8d allow an all-but-perfect reflectivity on a range of Δ greater than 100 nm (centred at Δ=350 nm). The triangular and rectangular lattices give similar results. 6 layers of air holes are required to obtain a reflectivity of more than 99 % and 10 layers ensure an all-but-perfect reflectivity (>99.99 %). Figures 2 show an excellent reflectivity of the photonic crystal in a wide spectral interval (>99.9 % over an interval of 200 nm) and high stability of the reflectivity according to the angle of incidence, given that the reflectivity is all but perfect for angles of incidence greater than 60°.

Reflected efficiencies in the –1st order are therefore studied as a function of the groove width and depth denoted respectively c and h in Fig.1. It can be seen in Fig.3 that these efficiencies can be numerically very high over wide intervals of h and c. Let us now study the reflection efficiency in the –1st order according to the angle of incidence and the incident wavelength (Figs. 4). The reflectivity of the crystal is insensitive to the incident wavelength and to angles of incidence greater than 60°, but the reflected efficiency in the –1st order is dependent upon that through the presence of the grating. The total reflected efficiency is always equal to 1, but part of the incident energy is diffracted in the 0th order [9]. The angular tolerance is good given that the reflected efficiency in the –1st order is greater than 99 % in an interval of 18 degrees. The spectral tolerance is comparable to that obtained with MLD gratings and imposed by the profile of the grating. The distribution of the electric field in the upper part of the grating (Fig. 5) is similar to that observed in MLD gratings as the field is concentrated in the grooves. An intensity enhancement can be observed at the right slope of the silica pillar, and recently it has been shown that the reduction of the pillars width permits to reduce this intensity enhancement in the silica and to increase the LIDT of the grating [4,13]. Moreover, no reinforcement of the field at the interfaces between air and silica is observed. Waddie et al. have shown that in the case of 2D photonic crystals made of square HfO_2 inclusions in a SiO_2 matrix, the maximum of the electric field occurs inside the HfO_2 inclusions, which increases the LIDT compared to MLD where the maximum of the electric field occurs at the interface between HfO_2 and SiO_2 [14]. But it is not the case when inclusions are made of low index material as it can be observed in Figure 5.

This study evidences that gratings composed solely of silica can offer reflected efficiencies in the –1st order greater than 99.9%. The reflectivity of the photonic crystal based on a contrast of refractive indices between air and silica is all but perfect over wide spectral intervals and angles of incidence. These results are valid in TE polarization and cannot be reproduced in TM polarization due to the poor reflectivity of the photonic crystal. Femtosecond laser micro-machining is the most adapted technique to manufacture two-dimensional photonic crystals in silica [15]. Afterward, the grating shall be manufactured by a classical holographic process. Effort are currently made to manufacture a first small size prototype by this mean. Moreover, being a laser machined and etched bare fused silica device, our prototype shall be fully compatible with vacuum exposition as in pulse compressors.

Bibliography

1. D. Strickland and G. Mourou, “Compression of amplified chirped optical pulses,” Opt. Commun. **56**, 219-221 (1985)
2. G. Loewen and E. Popov, *Diffraction Gratings and Applications* (Marcel Dekker, Inc, 1997)
3. M. D. Perry, R. D. Boyd, J. A. Britten, B. W. Shore, C. Shannon and L. Li, “High efficiency multilayer dielectric diffraction gratings,” Opt. Lett. **20**, 940-942 (1995)
4. J. Neauport, E. Lavastre, G. Raze, G. Dupuy, N. Bonod, M. Balas, G. de Villele, J. Flamand, S. Kaladgew, F. Desserouer, “Effect of electric field on laser induced damage threshold of multilayer dielectric gratings,” Opt. Express **19**, 12508-12522 (2007)
5. M. Mero, J. Liu, W. Rudlph, D. Ristau, K. Starke, “Scaling laws of femtosecond laser pulse induced breakdown in oxide films,” Phys. Rev. B **71**, 115109 (2005)
6. K. Sakoda, *Optical Properties of Photonic Crystals*, (Springer, Berlin, 2001)
7. E. Popov, B. Bozhkov, and M. Neviere, “Almost perfect blazing by photonic crystal rods gratings,” Appl. Opt. **40**, 2417-2422 (2001)
8. D. Maystre, “Photonic crystal diffraction grating,” Opt. Express **8**, 209-216 (2001)
9. N. Bonod, E. Popov, S. Enoch, J. Neauport, “Polarization insensitive blazed diffraction gratings,” J. Eur. Opt. Soc. RP **1**, 06029 (2006).
10. N. Blanchot, G. Marre, J. Neauport, C. Rouyer, S. Montant, A. Cotel, C. Leblanc, C. Sauteret, “Synthetic aperture compression scheme for multi-petawatt high energy laser,” Appl. Opt. **45**, 6013-6021 (2006)
11. R. Padjen, J. M. Gerard, J. Y. Marzin, “Analysis of the filling pattern dependence of the photonic bandgap for two-dimensional systems,” J. Mod. Opt. **41**, 295-310 (1994)

12. M. Neviere, E. Popov, *Light propagation in periodic medias ; differential theory and design*, (Marcel Dekker, New York, Basel, Honk Kong, 2003)

13. N. Bonod, J. Neauport, "Optical performances and laser induced damage threshold improvement of diffraction gratings used as compressors in high power lasers," Opt. Commun. **260**, 649-655 (2006)

14. A. J. Waddie, M. J. Thomson, M. R. Taghizadeh, "Comparison of one- and two-dimensional dielectric reflector geometries for high-energy laser pulse compression," Opt. Lett. **30**, 991-993, (2005)

15. V. Mizeikis, H. Sun, A. Marcinkevicius, J. Nishii, S. Matsuo, S. Juodkazis and H. Misawa, "Femtosecond laser micro-fabrication for tailoring crystals in resins and silica", J. Photochem. Photobiol. A: Chem. **145,** 41-47 (2001)

List of figures

Fig.1.

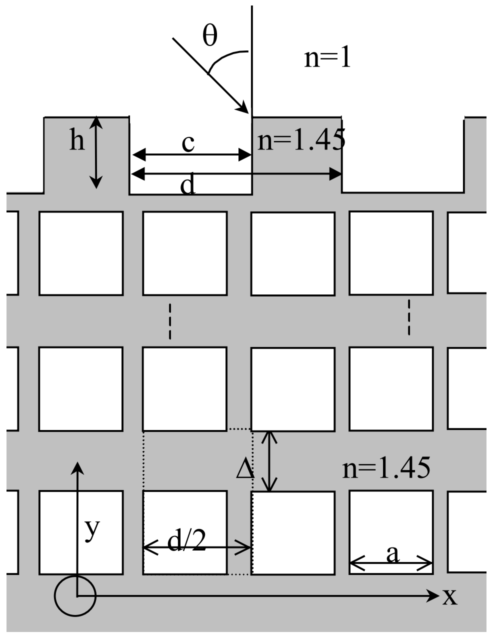

Figs.2.

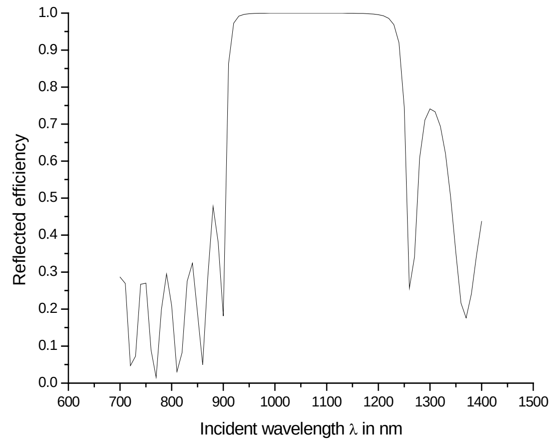
Reflected efficiency
1.0
0.9
0.8
0.7
0.6
0.5
0.4
0.3
0.2
0.1
0.0
600
700
800
900
1000
1100
1200
1300
1400
1500
Incident wavelength λ in nm

(a)

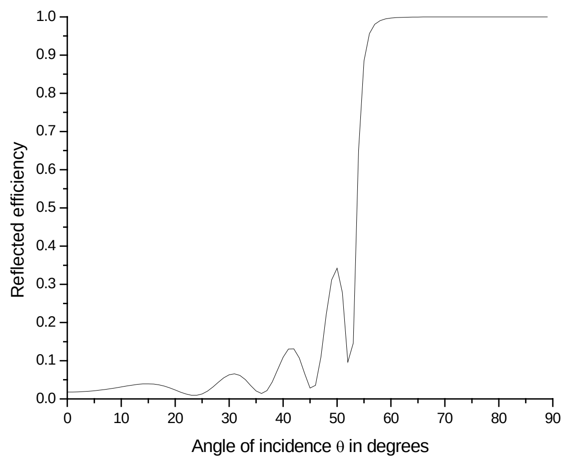
Reflected efficiency
1.0
0.9
0.8
0.7
0.6
0.5
0.4
0.3
0.2
0.1
0.0
0
10
20
30
40
50
60
70
80
90
Angle of incidence θ in degrees

(b)

Fig.3.

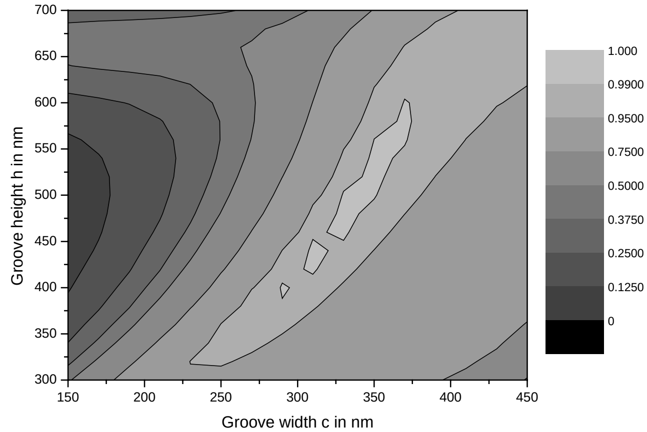

Groove height h in nm
Groove width c in nm
700
650
600
550
500
450
400
350
300
150
200
250
300
350
400
450
1.000
0.9900
0.9500
0.7500
0.5000
0.3750
0.2500
0.1250
0

Figs.4.

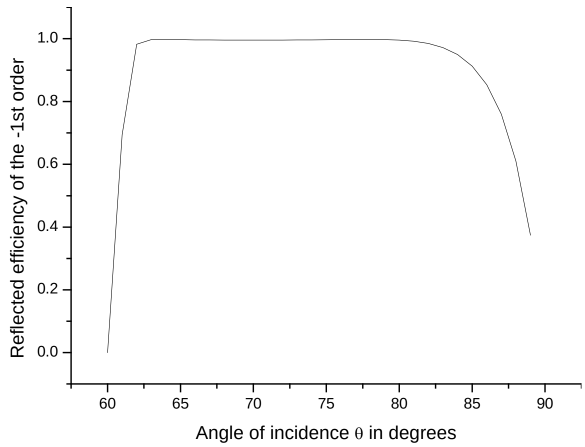

Reflected efficiency of the -1st order
1.0
0.8
0.6
0.4
0.2
0.0
60
65
70
75
80
85
90
Angle of incidence θ in degrees

(a)

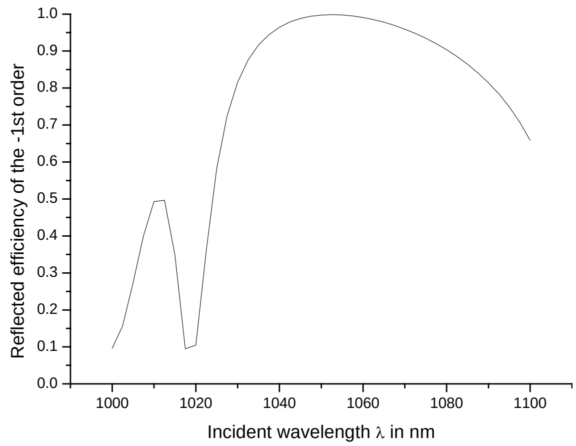

Reflected efficiency of the -1st order
1.0
0.9
0.8
0.7
0.6
0.5
0.4
0.3
0.2
0.1
0.0
1000
1020
1040
1060
1080
1100
Incident wavelength λ in nm

(b)

Fig.5

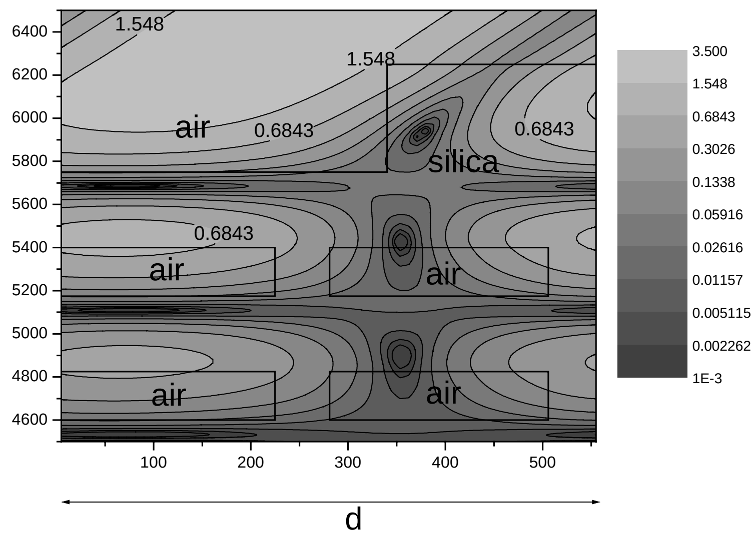

1.548
1.548
air
0.6843
0.6843
silica
0.6843
air
air
air
air
6400
6200
6000
5800
5600
5400
5200
5000
4800
4600
100
200
300
400
500
d
3.500
1.548
0.6843
0.3026
0.1338
0.05916
0.02616
0.01157
0.005115
0.002262
1E-3